

## Science-Driven Innovation: Developing the Right Tools for Solar Research

*Pietro N. Bernasconi, David M. Rust, Barry J. LaBonte, and Manolis K. Georgoulis*

**T**he goal of the APL solar physics research program is to deepen our understanding of the fundamental physical processes on the Sun. For this purpose we have built and tested innovative solar instruments and telescopes such as the Flare Genesis Experiment and the Solar Bolometric Imager. This article briefly describes the instrumentation program and then focuses on the scientific advances achieved through the flight test program. With the Flare Genesis Experiment, we found that magnetic flux emerges through the solar surface in relatively tiny strands that undulate with a characteristic wavelength of 3000 km. And the first flight of the Solar Bolometric Imager showed remarkable agreement between the measured contrast of features on the solar surface and a blackbody model. We plan to obtain a longer series of measurements that will allow detection of subtle large-scale surface temperature variations and their potential impact on total solar irradiance, which largely controls Earth's climate.

### INTRODUCTION

The science of solar physics concerns how the universal laws of physics apply to the Sun and, by extension, to all Sun-like stars. Our research focuses on the causes of solar variability. One of our current science goals is to find the link, if any, between the onset of solar flares and the emergence of magnetic fields into the outer solar atmosphere (the corona) from beneath the photosphere, which is the visible, gaseous surface of the Sun. A second science goal is to determine whether the known variations in solar output can be completely explained by sunspots and other fluctuations caused by the magnetic fields or whether other undiscovered mechanisms are acting in subtle ways that could have long-term consequences for Earth's climate.

Above all, solar physics is based on observations. The APL Solar Physics Section identifies new tools that most directly make the measurements required to achieve our science goals. Ideally, these tools would be used for spaceflight to avoid the effects of Earth's atmosphere. For the sensitive measurements we are trying to make, we must avoid the blurring and variable transparency of the Sun as viewed from the ground. The ideal test platform for space-bound instruments is the high-altitude balloon-borne gondola. In the upper stratosphere, 30–40 km above the ground, balloon flights provide near-space test conditions for extended periods at low cost. At APL, we have flown two innovative telescopes aboard balloon-borne gondolas in the past

5 years and are preparing for another flight. The technology innovations have, in turn, contributed strongly toward achieving two fundamental science goals in solar research: better understanding of solar flares and greater insight into the role of solar variability in driving global climate change.

APL has flown two distinctly different telescopes: the Flare Genesis Experiment (FGE) in January 2000 and the Solar Bolometric Imager (SBI) in September 2003. Both are prototypes of telescopes that NASA should fly in space eventually, but they differ in their science objectives and, therefore, in their design. Both programs are based on new technologies that are being tested for spaceflight. The successful demonstration of these technologies can be described in several ways. In this article, we focus primarily on how the flights have achieved their science objectives. We give only brief descriptions of the instrumentation; more details can be found in Refs. 1–4.

## FLARE GENESIS EXPERIMENT

### January 2000 Flight

The principal science goal of the FGE was to understand how the fibrous magnetic fields at the solar surface (the photosphere) emerge, coalesce, unravel, and erupt in solar flares. From a technology standpoint, the main goal was to demonstrate that lithium niobate Fabry-Perot etalon filters and liquid-crystal polarizers could be used in a vacuum environment to obtain reliable high-resolution maps of the photospheric magnetic fields. This goal was certainly achieved, as the science discussed below illustrates.

The FGE's focal-plane instrument was a filter vector magnetograph,<sup>1,2</sup> whose main components were a polarization analyzer package (two liquid-crystal variable retarders and a linear polarizer), a lithium niobate tunable Fabry-Perot etalon filter with a 0.016-nm passband,<sup>5</sup> and a 1024 × 1024 pixel high-speed CCD camera. The vector magnetograph was mated to an 80-cm telescope capable of mapping the strength and direction of the magnetic fields on the surface of the Sun with high spatial resolution (theoretically, 0.2 arcsec, ≈150 km on the Sun). It was the first vector magnetograph to fly in space or near-space.

In late October 1999, we deployed to the U.S. Antarctic base in McMurdo (76°S latitude), where we spent the next 2 months reassembling, testing, and calibrating the instrument. After waiting for favorable meteorological conditions, we finally successfully launched the FGE on 10 January 2000 (Fig. 1). Seventeen days later, after completing almost a full circumnavigation of the globe at about 78°S latitude and at a 36-km altitude, the FGE was brought down by parachute to the Ross Ice Shelf, about 320 km from McMurdo. Two weeks later we were



**Figure 1.** The Flare Genesis Experiment ready for launch in Antarctica, 10 January 2000.

able to reach the landing site and recover the onboard hard drives that stored all of the flight data. Because it was getting late in the season for Antarctic operations, it was not possible to return the telescope and its gondola to McMurdo. We had to leave it where it landed for the winter. One year later, the valiant Antarctic operations pilots and staff of the NASA-operated National Scientific Ballooning Facility recovered the full FGE gondola and payload and shipped it back to APL. More technical information about Flare Genesis instrumentation, as well as descriptions of our Antarctic expeditions can be found at our website: <http://sd-www.jhuapl.edu/FlareGenesis/>.

During its flight, the FGE recorded thousands of images in the three polarization states (two linear and one circular) of the incoming solar radiation. After the flight, we converted the images into maps of all three components of the photospheric magnetic field with a spatial resolution of ≈0.5 arcsec and a temporal cadence of 3.5 min. The data also included high-resolution Doppler maps showing the flow of the photospheric plasma along the line of sight. In addition to the photospheric magnetic and plasma flow maps recorded in a spectral line of atomic calcium at 612.2 nm, the FGE recorded images with the Fabry-Perot filter centered on the spectral line of atomic hydrogen at 656.3 nm, which is the so-called H $\alpha$  line. Observations at this wavelength show the structure and evolution of the chromosphere, a highly dynamic layer of gases just above the photosphere and typically extending to an altitude ranging from 1,000 to 10,000 km. In addition, FGE images were complemented by images obtained at many other wavelengths at cooperating ground-based and space-based observatories.

### Magnetic Structure in an Emerging Sunspot Region

On 25 January 2000, we commanded the FGE to point at an interesting “active region” (AR; a place where intense magnetic fields emerge from below the

photosphere) labeled National Oceanic and Atmospheric Administration (NOAA) AR 8844 (Fig. 2). A 4-h movie derived from the FGE observations shows that this region was growing quite rapidly: the two large sunspots of opposite magnetic polarity were moving apart with high speed, and at the center of the region, new magnetic flux was constantly emerging from below the photosphere.

The observations of NOAA AR 8844 revealed many tiny moving features with closely joined magnetic polarities. These features emerged in the center of large convection cells and quickly moved as single units toward the cells' edges. Similar features have been observed in the past but never in such detail. The previously reported features appeared at the periphery of decaying sunspots and moved away from the spots: they are generally thought to be part of the sunspot decay process. In our observations, most of the new poles moved toward the sunspots and were clearly part of the sunspot growth process. We called them "moving dipolar features"<sup>6</sup> (MDFs).

Figure 3 shows the evolution of two MDFs that drifted with an average speed of 0.4 km/s toward the negative polarity sunspot. Eventually the spot swallows one of them. It is interesting that the magnetic polarity of the MDF pole closest to the spot is opposite that of the spot itself. Furthermore, a close look at the direction of the magnetic field vectors (Fig. 4) clearly indicates that MDFs are U-shaped magnetic loops stitched into the upper photosphere and not the earlier observed  $\Omega$ -shaped loops (see also the sketch in Fig. 7b). MDFs look

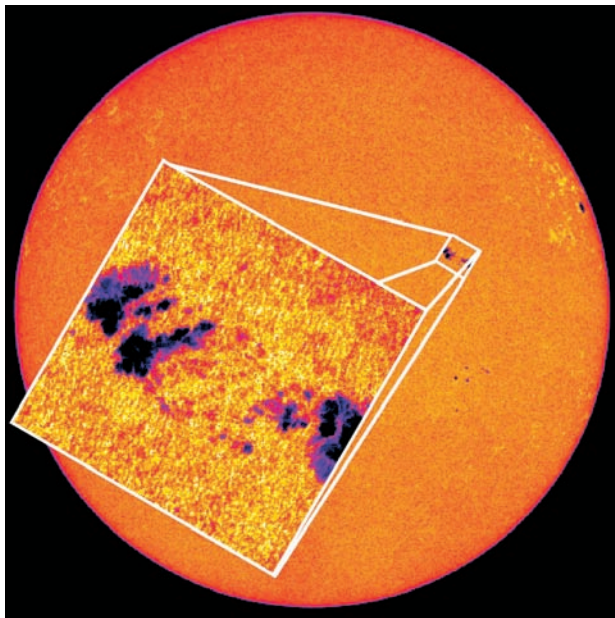


**Figure 2.** The Flare Genesis telescope obtained greatly magnified images of a rapidly growing sunspot region on 25 January 2000. The FGE field of view was  $90 \times 90$  arcsec. For comparison, the solar disk is 1920 arcsec in diameter.

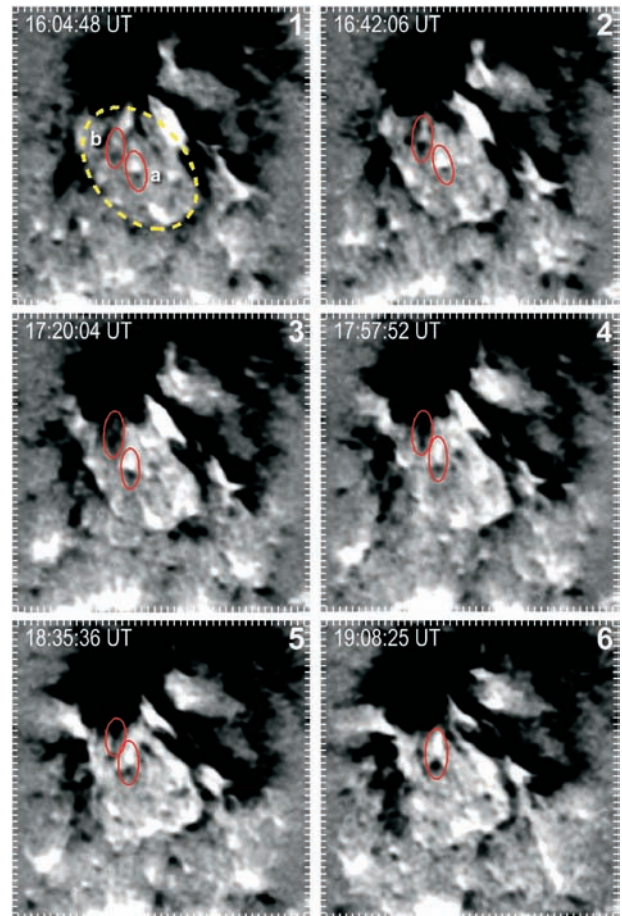


**Figure 3.** A sequence of magnetograms showing two MDFs (red ellipses marked "a" and "b" in frame 1) migrating toward the negative polarity spot of NOAA AR 8844 (black area at top). Most MDFs appeared in the convection cell indicated by the yellow dashed ellipse (frame 1). The MDF marked "b" gets swallowed into the sunspot. (Tick mark interval = 725 km.)

like little wiggling disturbances embedded in a sea of mostly horizontal magnetic field lines. And at the center of each of the two MDF poles, we found persistent flows of material downward into the photosphere. All MDFs are remarkably similar in size, field strength, and orientation of the vector magnetic field. This suggests that they are formed by an instability in the fields having a characteristic wavelength, in this case about 3000 km.<sup>6</sup>

Our interpretation of these observations is that MDFs form when plasma carried up through the photosphere flows downward from points at which the undulations in the magnetic field emerge first. These flows further distort the field lines, amplifying each concave depression in them. The bending of the field lines triggers the further flow of material toward the center of each depression, thus creating U-loops. Each newly formed MDF is swept by the horizontal outward flows within the convection cell toward the edge of the cell, where finally the entrained material can slide down into the sunspot. By revealing the characteristic size and undulation scale

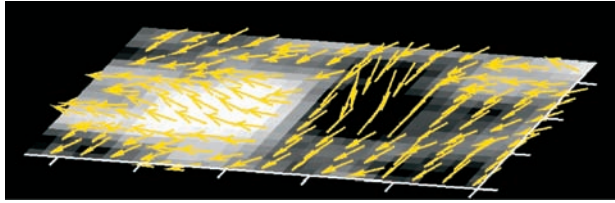


**Figure 4.** View in perspective of the magnetic field geometry of the MDF marked “a” in Fig. 3, which clearly exhibits a U-shaped magnetic structure.

of the magnetic field threads forming the sunspots, these FGE observations greatly improved our knowledge of the early evolutionary stages of solar ARs. Movies of these observations and relevant scientific articles can be found at <http://sd-www.jhuapl.edu/FlareGenesis/Science>.

### Heating the Active Region Corona

With support from the worldwide network of telescopes, we obtained simultaneous views of AR 8844 in many wavelengths, from the visible to soft X-rays (Fig. 5). The objective was to see the effect of AR growth on the overlying layers of the solar atmosphere. Our FGE observations showed that the region’s magnetic structure was quite fragmented (Fig. 5a), with strong magnetic flux accumulations distributed to spatial scales as small as the FGE’s spatial resolution ( $\approx 0.5$  arcsec or  $\approx 360$  km). If the spatial resolution had been higher, we believe we would have seen even smaller magnetic structures.

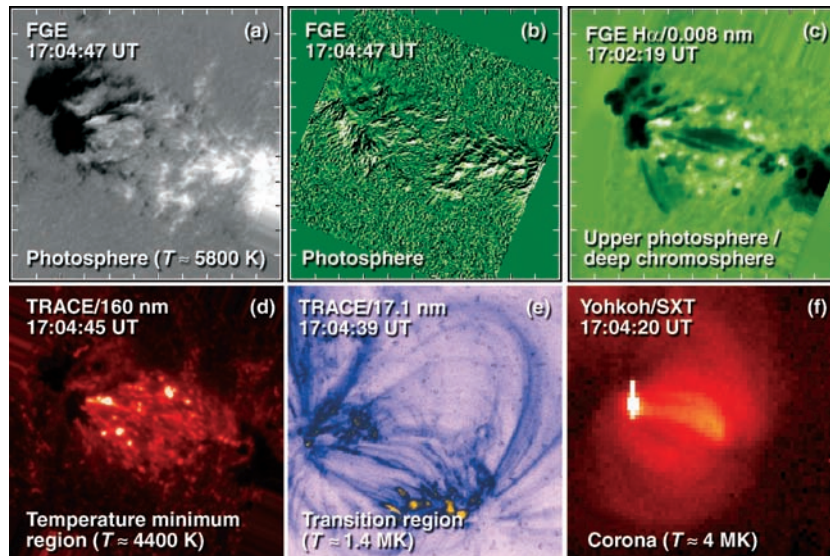


**Figure 5.** Multi-wavelength view of NOAA AR 8844 on 25 January 2000. (a) Vertical photospheric magnetic field, where white and black indicate upward and downward pointed fields, respectively. (b) Vertical component of the sheath current density calculated from the measured magnetic field vectors. (c) Off-band  $H\alpha$  filtergram showing Ellerman bombs (bright dots). (d) Deep chromosphere image at 160 nm. (e) EUV view of the transition region at 17.1 nm. (f) The soft X-ray emission from the overlying corona. Tick mark separation in a–c is 10 arcsec ( $\approx 7250$  km). The field of view is nearly the same for all six images.

Working from the measured magnetic field vectors on the photospheric level, we were able to calculate the vertical current density via Ampere’s law (Fig. 5b). Thus we found that the evolution of the magnetic fields in the photosphere creates extremely complex patterns of strong vertical currents. These current patterns clearly reveal the filamentary nature of the emerged magnetic fields, which induce a highly structured 3-D configuration of magnetic loops in the overlying solar corona. These loops are bright in various wavelengths, from the EUV produced at about 1 million K (Fig. 5e) to the soft X-ray region (Fig. 5f), which indicates the presence of 4 million K plasma. One of the greatest mysteries in solar physics is how the corona can be heated to such temperatures when the underlying photosphere is only 5000 K.

We constructed a complex picture<sup>7</sup> of the large-scale magnetic evolution in NOAA AR 8844 from images of the activity in the various layers of the atmosphere. We linked the gradual appearance of magnetic loops in the corona and the transition region between chromosphere and corona, where the temperature jumps from 5000 to 2 million K in about 5000 km (Figs. 5e, 5f) to the magneto-kinematic evolution of the corresponding magnetic dipoles on the AR photosphere. Using magnetic extrapolation techniques, we tracked and modeled the transition region and coronal loops and found that they do not coincide. They appear to have been formed independently (Fig. 6). The soft X-ray loops at 4 million K appeared 30–40 min before the EUV loops at 90,000 to 1.4 million K. The inter-

pretation of this timing, as well as the interrelation of soft X-ray and EUV emissions, is an issue of lively debate in solar physics. In terms of loop heating, we conclude that the EUV transition region loops are heated primarily near their footpoints, i.e., in low altitudes in the solar atmosphere. On the other hand, our results suggest that the coronal soft X-ray loops probably brighten in response to coronal magnetic reconnection.

The nature of energy release and heating in the solar atmosphere is the subject of intense investigation and debate. Two viewpoints have many adherents. One group believes in inhomogeneous, low-altitude heating whereas the other proposes homogeneous heating originating high in the corona. Our findings, arguing for different heating attributes for the two different types of emission, may be able to resolve the controversy.

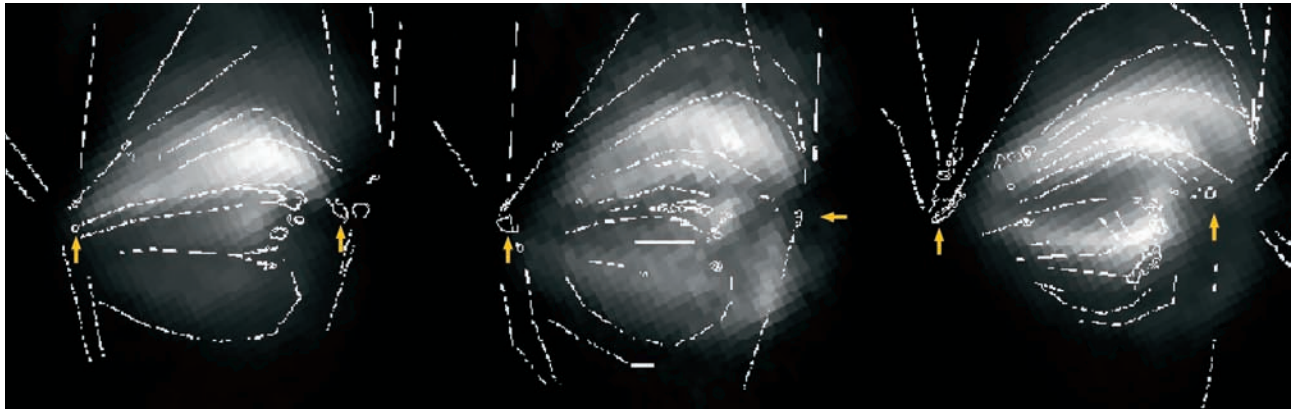


**Figure 6.** Co-alignment between soft X-ray loops (bright features) and nearly simultaneous EUV loops (represented by white dotted curves). The small contours indicated by the yellow arrows correspond to the calculated footpoints of the soft X-ray loops.<sup>7</sup>

### Magnetic Reconnection and Resistive Heating

As shown in Fig. 5c, the emergence of magnetic flux in NOAA AR 8844 was accompanied by large numbers of Ellerman bombs<sup>8</sup> (EBs), which are point-like brightenings in the lower chromosphere. Each bomb lasts about 10 min and may recur after 30 min. We performed a detailed morphological and statistical analysis of the EBs<sup>9</sup> and found that they share the physics of small solar flares, obeying self-similar distribution functions in their total and peak released energies and their durations. Typical energies of EBs were estimated in the range of  $10^{27}$  to  $10^{28}$  ergs, which is comparable to that of microflares or to 10–100 times the annual energy output of all the world’s nuclear power plants combined. Over the course of the FGE observations ( $\approx 3.5$  h), a total estimated energy of a few times  $10^{29}$  ergs was released in the form of EBs. This energy corresponds to the energy of an otherwise unobservable solar flare and, given the small spatial extent of our subject AR, it is evident that large numbers of EBs contribute significantly to the heating of the chromosphere in such regions.

Our analysis showed that EBs are manifestations of stochastic, low-altitude, magnetic reconnection in the solar atmosphere. The reconnection region was traditionally thought to be located in the magnetically dominated solar corona, but our observations and modern theoretical findings challenge this view. We infer that magnetic reconnection is ubiquitous in the upper photosphere/lower chromosphere

and may occur on magnetic separatrices and quasi-separatrix layers, which is where the connectivity of the magnetic field lines changes. Three likely structures featuring this type of discontinuity have been inferred from the FGE observations (Fig. 7).

Our first study of EBs was mainly observational, motivated by the observations acquired by the FGE and other space-based instruments. In a second phase, we attempted a deeper analysis based on the modeling of

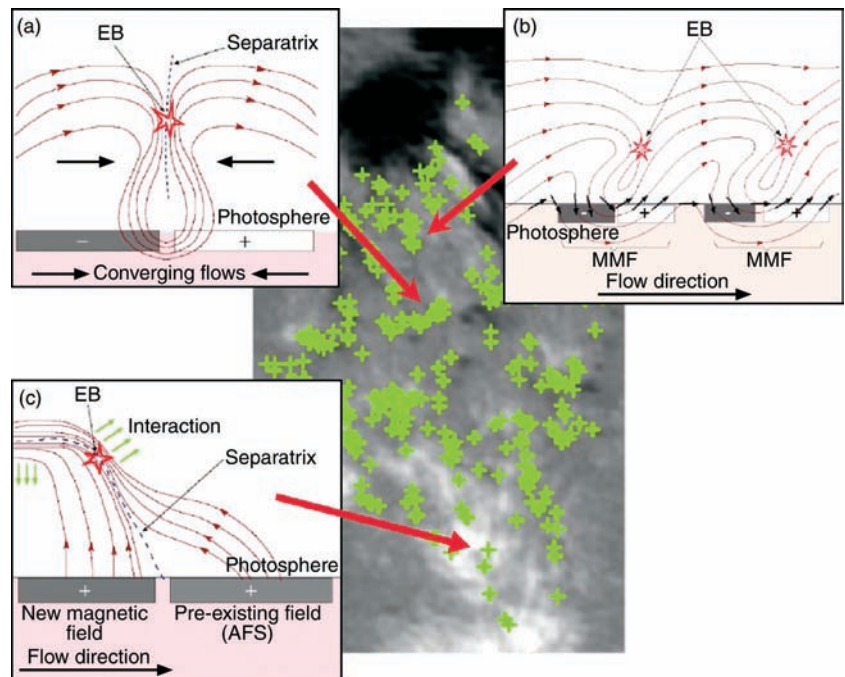


**Figure 7.** Physical interpretation of EBs as magnetic reconnection events occurring on magnetic separatrices and quasi-separatrix layers. The central image shows the vertical magnetic field of NOAA AR 8844, with black indicating negative fields and white indicating positive fields. The green crosses correspond to the mean locations of EBs over the course of the FGE observations. Three different situations for EB triggering have been found: (a) forced reconnection above a neutral line caused by converging photospheric flows, (b) reconnection above moving magnetic dipolar features<sup>6</sup> (MMF = moving magnetic features), and (c) reconnection between emerging and pre-existing magnetic field lines in a quasi-separatrix layer<sup>9</sup> (AFS = arch filament system).

the 3-D magnetic field vector in AR 8844. In Pariat et al.<sup>10</sup> we fitted the transition region loops with magnetic field extrapolations using the photospheric magnetic field measured by the FGE as the boundary condition (Fig. 8a). Our objective was to quantitatively study the flux emergence process by calculating the locations of magnetic separatrices, quasi-separatrix layers, and their photospheric signatures, the magnetic “bald patches” (BPs). These patches are areas where the magnetic field vector is tangent to the photospheric plane, while the surroundings show a concave magnetic field geometry.

To perform such a detailed topological analysis one needs exceptionally high-resolution magnetic field observations like those acquired by the FGE. From this topological analysis we found that the prevailing, traditional viewpoint of a smooth emergence of convex AR magnetic loops ( $\Omega$ -loops) into the solar atmosphere is fundamentally incomplete: the observed  $\Omega$ -loops are formed by the resistive emergence of undulatory flux ropes. The upper parts of the emerging flux ropes are significantly deformed and decelerated when reaching

the photosphere, thus creating a large number of BPs and localized concave emerging magnetic structures (U-loops; Figs. 8c, 8d). For these U-loops to fully emerge into the solar atmosphere, the action of magnetic reconnection (via resistive effects, i.e., energy dissipation in electric currents) is necessary. The relevant magnetohydrodynamical instability is the Parker instability,<sup>11</sup> which is triggered when the characteristic wavelength of the emerging magnetic field lines becomes larger than the photospheric pressure scale height. Thus, magnetic flux emergence is an inherently complex process characterized by a significant fragmentation of the magnetic flux bundles. The filamentary nature of the emerged magnetic flux causes this complexity. Moreover, we found that EBs largely coincide with either BPs or with the footpoints of the separatrix magnetic field lines (Fig. 8b), thus making EBs the signature of magnetic reconnection caused by the Parker instability or, in other words, the signature of the resistive emergence of undulatory flux ropes in the solar atmosphere. The study of Pariat et al.,<sup>10</sup> therefore, fitted the several dispersed pieces of the

flux emergence puzzle together into a coherent picture that reconciles flux emergence, magnetic reconnection, and heating in the solar atmosphere.

## SOLAR BOLOMETRIC IMAGER

### Is the Sun’s Output Constant?

The Sun is the dominant energy source controlling Earth’s climate. The generally accepted value for the total solar irradiance (TSI) integrated over all wavelengths arriving at the top of our atmosphere is  $1367 \text{ W/m}^2$ , which is also called the solar constant. During the past 26 years a series of space-based solar radiometers have delivered very precise measurements of the TSI, showing that it is far from being constant. This presented a fundamental question: Does the luminosity variation intrinsic to the Sun drive climate change on timescales relevant to the global warming problem?

The TSI varies by up to 0.5% day-to-day, mostly because of the passage across the visible solar disk of cool, dark sunspots and hot, bright areas called “faculae.” Analyses and modeling of the total irradiance record have shown that almost 90%

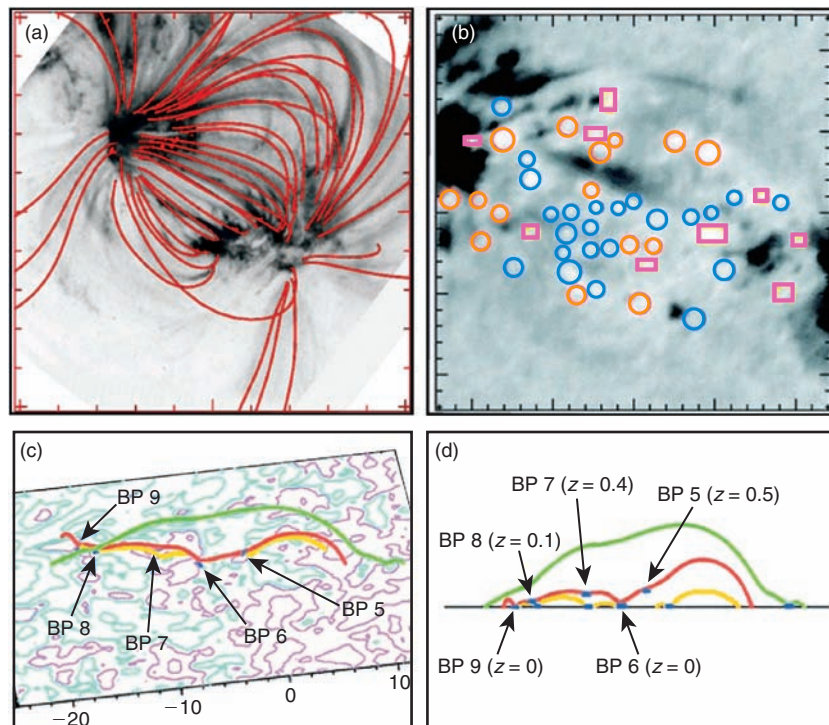


**Figure 8.** The complexity of magnetic flux emergence in the solar atmosphere. (a) Extrapolation of the FGE photospheric magnetic field vector to fit the observed magnetic configuration in the transition region. The extrapolated magnetic field lines are shown by the curves, while the image is an EUV view. (b) Spatial correlation between EBs and BPs/separatrices superposed on an FGE off-band  $H\alpha$  image of the region. The circles denote the locations of EBs that match the locations of BPs (blue) or the separatrix footpoints (orange). The rectangles denote the locations of EBs that cannot be matched by the above features. In this example, 38 out of 47 EBs ( $\approx 81\%$ ) can be matched by topological features likely to trigger magnetic reconnection via the Parker instability. (c) Detail of the magnetic flux emergence process showing a newly emerged magnetic field line (green) as well as two emerging lines (red and yellow) showing several U-loops and corresponding BPs. The contours correspond to the photospheric magnetic field strength. (d) A side view of Fig. 8c. (Reproduced with permission from Ref. 10; © 2004, AAS.)

of the TSI variation is well correlated with the expected changes resulting from sunspots and faculae coming and going. However, it is still not clear whether the photometric effect of these features actually equals or just simply is proportional to the measured radiometric fluctuations. The main problem is that space-based radiometers consider the Sun as a point source; therefore, they cannot provide any information on the localized sources of irradiance variation. Ground-based solar telescopes are of limited use because they can image only limited wavelength intervals. Until broadband imaging is available from space, it cannot be considered proven that changes in sunspots and faculae account entirely for the measured TSI variation. There could well be other processes not related to solar magnetism, as sunspots and faculae are, that play an important role in long-term solar irradiance variability. Unveiling these processes would help us to understand the Sun's role, if any, in global warming.

In collaboration with Peter Foukal of Heliophysics, Inc., APL developed the SBI,<sup>3,4</sup> an innovative solar telescope that can take images in light integrated over nearly the entire solar spectrum. The SBI's flat spectral response from the UV to the IR (like that of space-based radiometers) directly images the sunspot, facular, and magnetic network contributions to the TSI so that they can be evaluated, removed, and observed for more subtle sources of irradiance variation. The measurements should be carried out from space for at least half a solar cycle.

As a first step to test the instrument concept and to start gathering scientifically meaningful data, we developed a balloon-borne version of the SBI. Details can be found at <http://sd-www.jhuapl.edu/SBI/>.

### SBI Instrumentation

The SBI consists of a 30-cm-aperture  $f/12$  Dall-Kirkham telescope feeding a thermal detector array of  $320 \times 240$  elements.<sup>4</sup> The telescope primary and secondary Pyrex mirrors are uncoated, first to reduce the sunlight to the level suitable for the detector, and second because of the favorable reflection properties of bare Pyrex. The resulting spectral transmission of the telescope is flat to within  $\pm 7\%$  from 0.28 to 2.60  $\mu\text{m}$ . The detector is an array of ferroelectric thermal IR elements modified by deposition of a thin coat of gold-black (a colloidal form of gold that exhibits excellent photon absorption characteristics). Radiation hitting the detector is uniformly absorbed, and its energy is redistributed by the gold-black as thermal emission. The thermal emission is detected by the underlying thermal IR barium-strontium-titanate imaging array to produce an essentially flat response across all wavelengths from the UV to beyond 10  $\mu\text{m}$  in the IR.

The balloon-borne SBI provides the first opportunity to image the Sun in evenly weighted *broadband*

light between about 0.31  $\mu\text{m}$  (set by the atmospheric transmission at balloon altitude) and 2.60  $\mu\text{m}$  (set by the absorption of a quartz window in front of the detector array). This spectral interval contains approximately 94% of the total solar radiation. The angular resolution of the instrument is approximately 5 arcsec, which is adequate to separate spots, faculae, and the magnetic network from nonmagnetic cell interiors. The SBI does not provide absolute measurements of the solar irradiance, but rather measurements of the broadband photometric contrast of localized structures relative to their surroundings in the quiet photosphere. These measurements require neither absolute calibration nor long-term reproducibility. Because of the relatively small size of the detector array, the actual field of view of the instrument is only  $917 \times 687$  arcsec, and to obtain a full image of the Sun ( $\approx 960$  arcsec in diameter), it is necessary to create a mosaic image with the telescope pointing at 10 different locations on the solar disk. The detector frame rate is 30 Hz, and 60 frames co-added (i.e., an effective integration time of 2 s) are sufficient to lower the noise ratio well below the "solar noise" induced by the Sun's 5-min oscillations.

We retrofitted the FGE gondola to accommodate the SBI telescope and electronics and replaced the FGE solar panel power system with batteries, which are more appropriate for a 1-day flight. In addition, we updated and improved several other payload subsystems inherited from the FGE project, such as the pointing and computer commanding systems.

### September 2003 Flight

After considerable testing and planning, we transported the payload to the NASA-operated National Scientific Ballooning Facility in Fort Sumner, New Mexico, and on 1 September 2003, we had a very successful 10-h flight at an average altitude of  $\approx 33$  km (109 kft). All the systems performed well and we captured more than 500,000 bolometric images of the Sun, with a precision matched only by nonimaging space-based radiometers. The flight provided important engineering data to validate the spaceflight reliability of the gold-black thermal array detector, and it verified the optical and thermal performance of the SBI's uncoated optics in a vacuum environment.

### Science Results

Figure 9 shows a full-disk image of the Sun in broadband light created from 10 images recorded during the 1 September 2003 flight. Each image is the average of 60 frames recorded at the same location and precisely co-aligned. The SBI took about 7.5 min to acquire all the images necessary to create this mosaic. Most of the time was spent changing the telescope pointing and then waiting for the induced pointing oscillations to

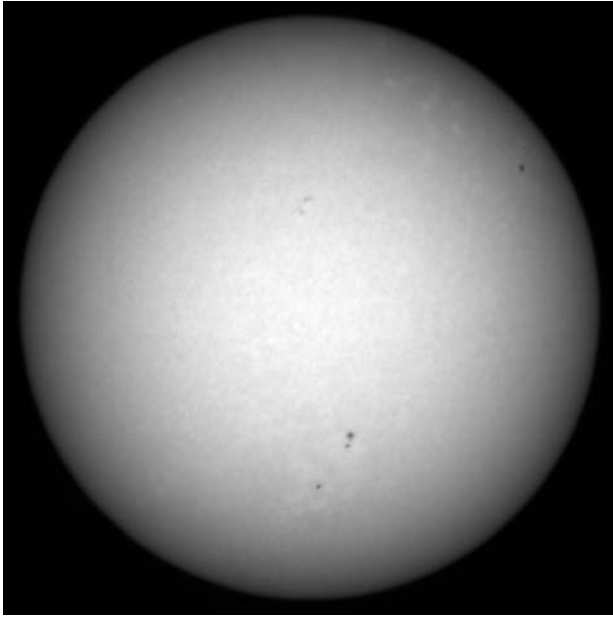


**Figure 9.** Full-disk mosaic of the Sun in bolometric contrast recorded by the SBI during the 1 September 2003 flight.

die down. Figure 9 represents the first image of the solar bolometric contrast ever recorded.<sup>12</sup> The so-called limb darkening dominates the image. The Sun's intensity is lower at the limb (edge) than at the center because at the limb our line of sight traverses more of the cool, upper layers of solar atmosphere, which are darker than the underlying photosphere. Nobody has ever before measured the center-to-limb variation of the solar intensity integrated over all wavelengths. Our observations agree well with theoretical and empirical predictions of the broadband limb-darkening curve.<sup>12</sup>

An important result of the SBI balloon flight is a first actual measurement of the bolometric center-to-limb variation of the photospheric contrast of the faculae and magnetic network. The contrast between faculae and their surroundings increases for faculae closer to the limb. Determination of the facular contrast curve has always been elusive because of the lack of truly broadband images of the solar photosphere. Knowing this curve with good accuracy is critical when trying to model the observed daily and long-term variation of the TSI.

We identified the location of the faculae and enhanced network on a full-disk image recorded with a filter centered on the Ca II K chromospheric line (at 390 nm) at the San Fernando Observatory with a telescope having a resolution similar to the SBI. The image was taken at the same time when the SBI was recording the broadband mosaics. In Ca II K images, faculae appear distinctively bright, making their identification easy. We located the identified faculae and enhanced network on the SBI intensity mosaic, and by considering all the pixels lying within the identified areas, we built a curve

of the average facular contrast (intensity normalized with respect to the immediate surroundings) versus distance from the Sun's center, expressed as  $\mu$ —the cosine of the heliocentric angle<sup>12</sup> (Fig. 10).

Our most interesting finding is the remarkable agreement between the SBI curve and a bolometric contrast curve estimated using a simple blackbody correction to the monochromatic facular contrasts measured at a similar angular resolution by Lawrence.<sup>13</sup> In this correction, it is assumed that the facular spectral radiation distribution is roughly similar to the emission distribution of a blackbody. The monochromatic contrast in a green (524.5-nm) or red (626.4-nm) passband having of width of 0.15 nm was used to calculate the facular blackbody temperature from the Planck function. The temperature was then used to compute the broadband blackbody radiation at this temperature. Also shown in Fig. 10 is a similarly corrected curve based on monochromatic measurements taken with a solar telescope at the San Fernando Observatory on the day of our balloon flight, in a 10-nm passband at 672 nm, and at a comparable angular resolution (personal communication, S. Walton, San Fernando Observatory). The similarity in both amplitude and shape of these three curves supports the validity of a blackbody approximation to facular radiative excess, at least to the accuracy required for irradiance modeling.

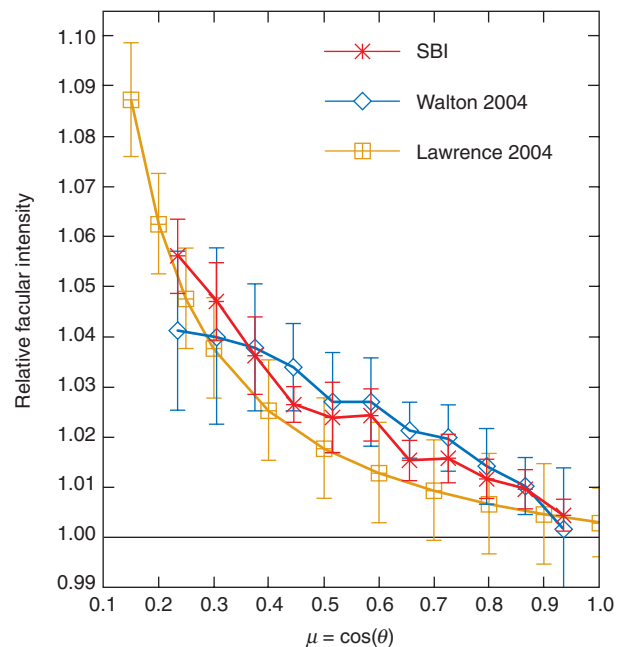


**Figure 10.** Asterisks: facular contrast measured by the SBI in integrated light versus the cosine of the angular distance from the Sun's center  $\mu$ . Diamonds: the equivalent red monochromatic measurements, obtained by S. Walton at the San Fernando Observatory, of the same faculae measured by the SBI on 1 September 2003. Squares: the bolometrically corrected monochromatic measurements of Lawrence.<sup>13</sup>



These results indicate that the SBI can take solar images that will allow us to remove the effects of sunspots and other magnetically controlled features and undertake a search for so-far undetected, subtle variations of a fundamental nature. To be successful, our search must be done from space or near-space because terrestrial weather and sky transparency variations make ground-based observations too noisy.

### SBI to Fly in Antarctica

After SBI's successful 1-day flight, we started a program to prepare the instrument for a longer balloon mission of 10 to 40 days in Antarctica. The flight is scheduled for December 2006, when solar activity will be near the minimum of its 11-year cycle. The main objective of this new mission is to understand the physical mechanisms of long-term solar variability. At solar minimum, the surface solar magnetic fields are at their weakest levels, and this will facilitate searching for and studying thermal structures that are not related to solar magnetism. Predicted and indirectly inferred structures, such as global torsional waves, meridional flows, and giant convective cells, have thermal signatures too weak to be detected with conventional techniques. The discovery of thermal signatures from these or other unsuspected sources would open a new era in understanding TSI variations because long-term changes would most likely be due to large-scale features.

## FUTURE MISSIONS

### ISIS

The logical follow-on to the balloon-borne SBI is a space-based Investigation of the Sources of Irradiance Variation on the Sun (ISIS), which would provide the first precise, wavelength-integrated photometric measurements of solar radiance variations over a substantial fraction of a solar cycle. Because of the stability that can be achieved with solar telescopes in space, the ISIS would be able to achieve unprecedented sensitivity. In terms of the temperature differences in the corresponding surface elements, the ISIS would be able to determine the relative temperatures of sunspots and faculae to within 8 K and the temperatures in large-scale patterns—such as might be expected in torsional waves, meridional flows, and giant convective cells—to within 1 mK.

### NICO

In the framework of developing new mission concepts, we recently proposed the Near Infrared Chromosphere Observatory (NICO). NICO would be a long-duration Antarctic balloon mission along the lines of the FGE. Its primary science objective would be to reveal the chromosphere's magnetic connection to the solar photosphere (Fig. 11). The interface between the two layers is called the magnetic transition region and is poorly understood. Moreover, single-height (i.e., photospheric) vector magnetic field measurements are ambiguous in the orientation of the transverse magnetic field component. NICO will obtain the photospheric and chromospheric vector magnetograms necessary to resolve this ambiguity definitively.

Another objective is to understand the elevation of mass from the photosphere to the chromosphere. The chromosphere is not in hydrostatic equilibrium, and the potential gravitational energy far exceeds the thermal energy content. Nevertheless, photospheric material is supplied to the chromosphere at an extremely high rate. The high spatial resolution and the multi-wavelength coverage of NICO can contribute to an understanding of the various chromospheric jets.

The third objective of NICO is to understand chromospheric heating. As noted previously, coronal heating is one of the inextricable puzzles in solar physics, but one cannot obtain a hot corona without a hot chromosphere. Despite the much smaller chromospheric temperature, of the order of  $10^4$  K (the corona has a mean temperature of  $\approx 2 \times 10^6$  K), the much denser

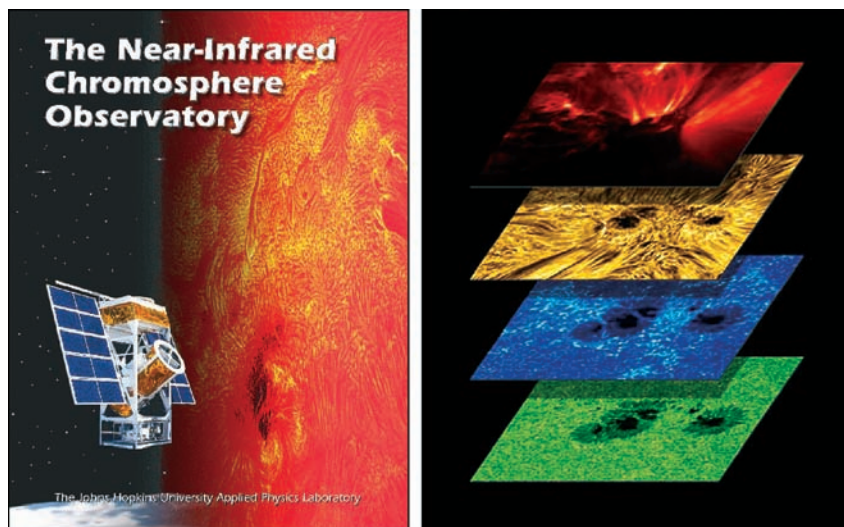


**Figure 11.** The concept of NICO (left) and its main objective, given schematically (right). NICO is a balloon-borne observatory. Its primary objective is to measure the physical conditions of the unexplored solar chromosphere (the yellow layer on the right) and to understand the connection between the chromosphere and the photosphere (blue and green layers) below. Understanding the chromosphere should help resolve one of the great puzzles of modern solar physics: How is the corona (red layer) heated to millions of degrees?

chromospheric material needs an energy input  $\approx 10$  times larger than that of the quiet corona to sustain its temperature. Without a hot chromosphere, the corona would disappear in a few hours. NICO can resolve both quiescent and active chromospheric structures to find signatures of magnetic reconnection. Moreover, it can detect relevant chromospheric wave modes and establish connections between them and chromospheric heating.

The means to achieve these goals are unique multi-wavelength observations with a sufficiently large field of view and very high spatial and temporal resolution. The chosen spectral lines reflect both photospheric and chromospheric emission: K I at 769.9 nm; Fe I at 868.8 nm (photospheric lines); the Ca II triplet at 849.8, 854.2, and 866.2 nm; He I at 1083 nm; and H $\alpha$  at 1083 nm (chromospheric lines). Measurement in these spectral lines will contribute chromospheric and photospheric vector magnetograms with a 100-arcsec ( $\approx 72,500$  km) field of view, a projected spatial resolution of 0.3 arcsec ( $\approx 220$  km), and sensitivity exceeding 20 and 70 G for the photosphere and chromosphere, respectively. The cadence of the above vector magnetograms exceeds 1 min. In addition, NICO will obtain the photospheric and chromospheric Doppler velocity with accuracy better than 5–10 m/s.

Besides its scientific contribution, NICO can be a cost-effective test bed for future space missions by demonstrating the use of technologies never before incorporated in space-borne telescopes. Some of these technologies include wavefront sensing for monitoring telescope alignment, high-speed image motion compensation, and wide-aperture, highly tunable Fabry-Perot etalon filters for extended spectral scanning.

## CONCLUSION

The APL solar flight program continues to make significant contributions to instrument development and solar research. The FGE was the first to measure the full magnetic field vector on a balloon-borne or space-based mission. The SBI made the first bolometric measurements of the solar surface. Looking to the future, we are planning a 10- to 40-day flight of the SBI to observe the Sun during the upcoming lull in magnetic activity, which may cloak subtle but important sources of irradiance variation. A multi-year investigation with ISIS is also possible. Although it is unlikely that a solar telescope the size of the FGE will be launched in space anytime soon, NICO can be operating by the next solar maximum, around 2011, since the payload can fly within 3 years of the mission's initial approval and funding. The technology of tunable

lithium niobate etalons, used successfully on the FGE, also makes possible a new generation of miniature vector magnetographs expected to fly on missions such as Solar Orbiter and Solar Probe over the next decades.

**ACKNOWLEDGMENTS:** The Flare Genesis data analysis was greatly aided by the cooperation of many observatories, especially NASA's Transition Region and Coronal Explorer (TRACE) and the Japanese Institute of Space and Astronautical Sciences (ISAS)/NASA Yohkoh Solar X-ray Telescope (SXT). We are also grateful to the staff of the National Scientific Ballooning Facility, which is operated for NASA by the Physical Sciences Laboratory of New Mexico State University. NASA grants funded most of the work described in this article. We thank Harry Eaton, lead APL engineer on the FGE and SBI projects, and Peter Foukal of Heliophysics, Inc., who played a key role in developing the SBI and interpreting its results. This article is dedicated to Barry J. LaBonte, who died shortly after it was completed.

## REFERENCES

- <sup>1</sup>Bernasconi, P. N., Rust, D. M., Murphy, G. A., and Eaton, H. A. C., "High Resolution Polarimetry with a Balloon-Borne Telescope: The Flare Genesis Experiment," in *High Resolution Solar Physics: Theory, Observations, and Techniques*, Vol. 183, T. R. Rimmele, K. S. Balasubramanian, and R. R. Radick (eds.), Astron. Soc. Pacific Conf. Ser., Sunspot, NM, pp. 279–287 (1999).
- <sup>2</sup>Bernasconi, P. N., Rust, D. M., Eaton, H. A. C., and Murphy, G. A., "A Balloon-borne Telescope for High-Resolution Solar Imaging and Polarimetry," in *Airborne Telescope Systems*, Vol. 4014, R. K. Melugin and H.-P. Roeser (eds.), SPIE, Munich, pp. 214–225 (2000).
- <sup>3</sup>Foukal, P., and Libonate, S., "Total-light Imager with Flat Spectral Response for Solar Photometric Measurements," *Appl. Opt.* **40**, 1138 (2001).
- <sup>4</sup>Bernasconi, P. N., Eaton, H. A. C., Foukal, P., and Rust, D. M., "The Solar Bolometric Imager," *Adv. Space Res.* **33**, 1746–1754 (2004).
- <sup>5</sup>Rust, D. M., "Etalon Filters," *Opt. Eng.* **33**, 3342–3348 (1994).
- <sup>6</sup>Bernasconi, P. N., Rust, D. M., Georgoulis, M. K., and LaBonte, B. J., "Moving Dipolar Features in an Emerging Flux Region," *Solar Phys.* **209**, 119–139 (2002).
- <sup>7</sup>Schmieder, B., Rust, D. M., Georgoulis, M. K., Démoulin, P., and Bernasconi, P. N., "Emerging Flux and the Heating of Coronal Loops," *Astrophys. J.* **601**, 530–545 (2004).
- <sup>8</sup>Ellerman, F., "Solar Hydrogen 'Bombs,'" *Astrophys. J.* **46**, 298 (1917).
- <sup>9</sup>Georgoulis, M. K., Rust, D. M., Bernasconi, P. N., and Schmieder, B., "Statistics, Morphology, and Energetics of Ellerman Bombs," *Astrophys. J.* **575**, 506–528 (2002).
- <sup>10</sup>Pariat, E., Aulanier, G., Schmieder, B., Georgoulis, M. K., Rust, D. M., and Bernasconi, P. N., "Resistive Emergence of Undulatory Flux Tubes," *Astrophys. J.* **614**, 1099–1112 (2004).
- <sup>11</sup>Parker, E. N., "The Dynamical State of the Interstellar Gas and Field," *Astrophys. J.* **145**, 811 (1966).
- <sup>12</sup>Foukal, P., Bernasconi, P. N., Eaton, H. A. C., and Rust, D. M., "Broadband Measurements of Facular Photometric Contrast Using the Solar Bolometric Imager," *Astrophys. J.* **611**, L57–L60 (2004).
- <sup>13</sup>Lawrence, J. K., "Multi-color Photometric Observations of Facular Contrasts," *Solar Phys.* **116**, 17–32 (1988).

## THE AUTHORS

**Pietro N. Bernasconi** served as the Project Scientist on both the FGE and the SBI. Dr. Bernasconi is a member of the APL Senior Professional Staff in the Space Department. He has extensive experience in the analysis of solar vector magnetic field measurements obtained from ground-based and balloon-borne telescopes. He is leading the further development of the SBI for Antarctic flight. **David M. Rust** leads the Space Department's Solar Physics Section and is the Principal Investigator on the FGE and SBI programs. Dr. Rust is an APL Principal Professional Staff member and an expert on solar telescopes and instrumentation. He has been an instructor in the Johns Hopkins Whiting School of Engineering, the University of Maryland, and The Catholic University of America. **Barry J. LaBonte**, who died tragically on 24 October 2005 of complications following surgery, led the Solar Physics Section's efforts to calculate the helicity flux in solar active regions and our efforts to automate solar event detection. Dr. LaBonte was a member of the Principal Professional Staff. Before coming to APL, he was Professor of Astronomy at the University of Hawaii. **Manolis K. Georgoulis** is a member of the APL Senior Professional Staff and the Principal Investigator on a study of mechanisms to heat the solar atmosphere. Dr. Georgoulis has published extensively on the statistical properties and magnetic field configurations involved with energy release in emerging and evolving active regions. Further information on the work of the experimental programs can be obtained from Pietro Bernasconi. His e-mail address is [pietro.bernasconi@jhuapl.edu](mailto:pietro.bernasconi@jhuapl.edu).



Pietro N. Bernasconi



David M. Rust



Barry J. LaBonte



Manolis K. Georgoulis